Manipulation of droplets and bubbles for thermal applications

Xichen Liang[1], Vijay Kumar[2], Farzad Ahmadi[2], Yangying Zhu[2]*
1 Department of Chemical Engineering, University of California, Santa Barbara, CA 93106
2 Department of Mechanical Engineering, University of California, Santa Barbara, CA 93106
* Corresponding author email: yangying@ucsb.edu

Abstract: Liquid-vapor phase change including evaporation, boiling and condensation is a ubiquitous process found in power generation, desalination, thermal management, building heating and cooling, and additive manufacturing. The dynamics of droplets and bubbles during phase change including nucleation, growth, and departure critically influence the thermal transport performance and system efficiency. This review will highlight recent advancements using static and dynamic strategies to manipulate droplets and bubbles for phase change applications and beyond.

Keywords: dynamic manipulation, droplets, bubbles, wettability, heat transfer, thermal applications

Introduction

Liquid-vapor phase change is a key process in various engineering and industrial applications because it harnesses the high latent heat of vaporization to efficiently transport thermal energy. For example, power plants utilize boiling to transport heat from the energy sources to produce electricity and rely on condensation to reject waste heat to the environment.[1] Improving the phase change heat transfer directly translates to improved efficiency of the power plant. A 1% increase in the power plant efficiency will lead to approximately 0.3 EJ/yr energy savings in the U.S. accompanied by reduced CO_2 emission.[2] Other applications include building space heating and cooling which consumes about 40% of total building energy consumption, electronics cooling, desalination, thermal diode, and additive manufacturing (**Figure 1a**).

Liquid-vapor phase change refers to evaporation, boiling, and condensation processes. In boiling and condensation, the nucleation, growth, and departure of vapor bubbles and droplets critically affect the heat transfer characteristics (**Figure 1b**).[3] These bubble and droplet dynamics are heavily influenced by surface wettability and morphology. In boiling, hydrophobic spots or cavities facilitate vapor nucleation by lowering the activation energy, and hydrophilic surfaces promote bubble departure by lowering the contact angle and thereby the net surface tension pinning force. Engineered surfaces that promote bubble nucleation can demonstrate the earlier onset of nucleate boiling (ONB) and an enhanced heat transfer coefficient (HTC), which is a measure of the effectiveness of heat transfer. On the other hand, superhydrophilic surfaces that promote capillary wetting and bubble departure have achieved over 200% enhancement in the critical heat flux (CHF) (**Figure 1c**).[3] Similarly, condensation surfaces that promote condensate removal through nanostructured superhydrophobic coatings have demonstrated significant heat transfer enhancement as well. Phase change heat transfer performance is usually characterized using a heat flux vs superheat/subcooling plot, as shown in **Figure 1c**. Superheat and subcooling are the difference in the wall temperature and the saturation temperature of the fluid for boiling and condensation, respectively. A desired characteristic curve would exhibit high HTC, high CHF, and early ONB. This would require engineering approaches to promote bubble/droplet nucleation, growth, and departure. On the contrary, a surface that suppresses nucleation and pins bubbles/droplets would show a poor heat transfer performance with reduced HTC and CHF. It can be seen that manipulating bubble and droplet dynamics is key to achieving enhanced and tunable thermal transport. Beyond phase change thermal transport, manipulation of droplets and bubbles enables new functionalities and performance enhancements in many other applications such as bubble departure in electrocatalysis[4–6], digital microfluidics[7], programmable micro-reactors[8], thermal diode[9,10], and micro-robots[11].

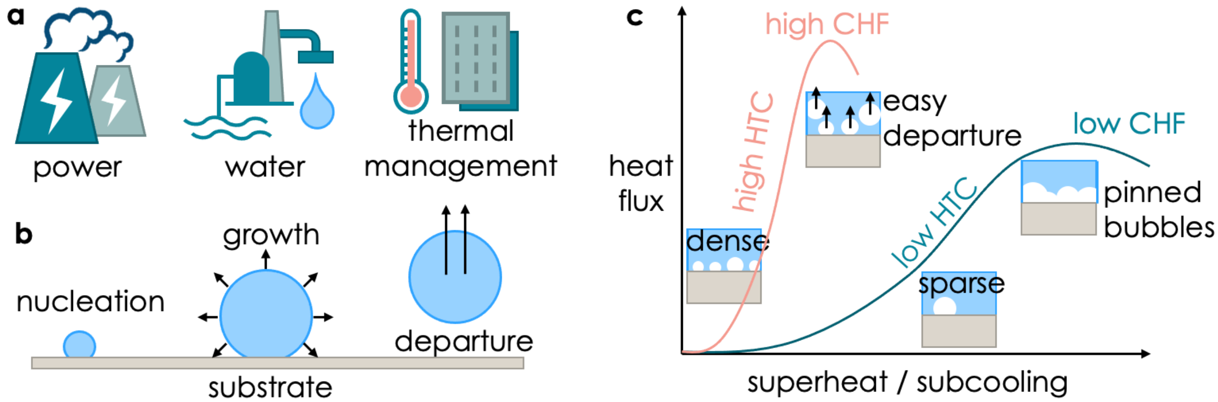

Figure 1. Droplet and bubble dynamics critically influence phase-change thermal transport. a, Applications of phase change heat transfer. b, Nucleation, growth, and departure of a droplet or bubble. c, Phase-change thermal transport figure of merit: heat flux vs superheat in boiling or subcooling in condensation. Easy bubble or droplet departure enhances the critical heat flux (CHF), while pinned bubbles or droplets lower the CHF. In addition, dense nucleation sites improve the heat transfer coefficient (HTC).

This review article will highlight recent developments using static (passive) and dynamic (active) approaches to tune the nucleation, growth, and departure behaviors of bubbles and droplets for heat transfer enhancement in thermal applications and related microfluidics applications. We will first review passive methods to manipulate thermal transport including asymmetric structures and chemistry, engineered nucleation sites, coalesce-induced jumping droplets, and slippery liquid-infused porous surfaces (SLIPS) surfaces for droplet removal. These passive approaches generally involve engineering static surface morphologies with nanometer to millimeter feature sizes and surface chemistry such as coatings to manipulate wetting behavior, therefore, impacting bubble and droplet dynamics. We will then introduce dynamic and active approaches to manipulate multi-phase thermal transport using electrowetting, electrostatic charging, and ionic and photo-responsive surfactants. The response timescale, stability, and energy requirements for each method will be discussed.

Static surface structures and chemistry

Asymmetric structures and chemistry

Asymmetric surface micro and nanostructures have been developed to direct liquid droplets or bubbles in a preferred direction by generating unbalanced surface tension forces (**Figures 2 a-c**).[12–18] For example, Chu et al. demonstrated uni-directional liquid spreading on tilted hydrophilic nanowires by tuning the contact angle and the geometry of nanowires (**Figures 2a and d**).[12] In the tilting direction of the nanowires, liquid wets the entire nanowire once it contacts the base of the nanowire, promoting the contact line to advance to the next row of pillars. In the opposite direction, the contact line stays pinned. More recently, Feng et al. designed a 3-dimensional asymmetric surface that selects liquid spreading directions based on its surface tension (**Figure 2e**).[16] Fast droplet transport has been demonstrated on curvature-gradient surfaces[17] and asymmetric hierarchical micro and nanostructured surfaces.[18]

In thermal applications, it is desired to remove liquid droplets or bubbles quickly from the substrates, which allows new droplets and bubbles to nucleate to achieve a continuous high heat flux. Buoyancy or gravity is usually the driving force for bubble and droplet departure. However, in the microgravity environment where buoyancy or gravity is absent, bubbles and droplets need to be removed via external forces to sustain the continuous phase change process. Asymmetric structures have successfully been demonstrated to directionally transport droplets and bubbles during phase change in both terrestrial and microgravity conditions. For example, ratchet surfaces have been shown to propel Leidenfrost droplets [19–21] with a velocity above 1 m/s (**Figure 2b, f**) in a controlled direction. The Leidenfrost effect refers to the levitation of a liquid droplet on a hot surface by an evaporating vapor layer. The asymmetric surfaces lead to a net propulsion force exerted by the vapor on the droplet. In condensation, asymmetric micropillars or microstructures can also drive the condensed liquid to move in a preferred direction [22–24]. For example, Park et al. designed a beetle-inspired surface with asymmetric bumps to initiate condensation preferentially on the top of the bump, and the condensed droplets spontaneously slide down the bump due to surface energy minimization.[22] Similarly, vapor bubbles can move on asymmetric surface structures in the absence of buoyancy during boiling (**Figure 2c, g**).[25]

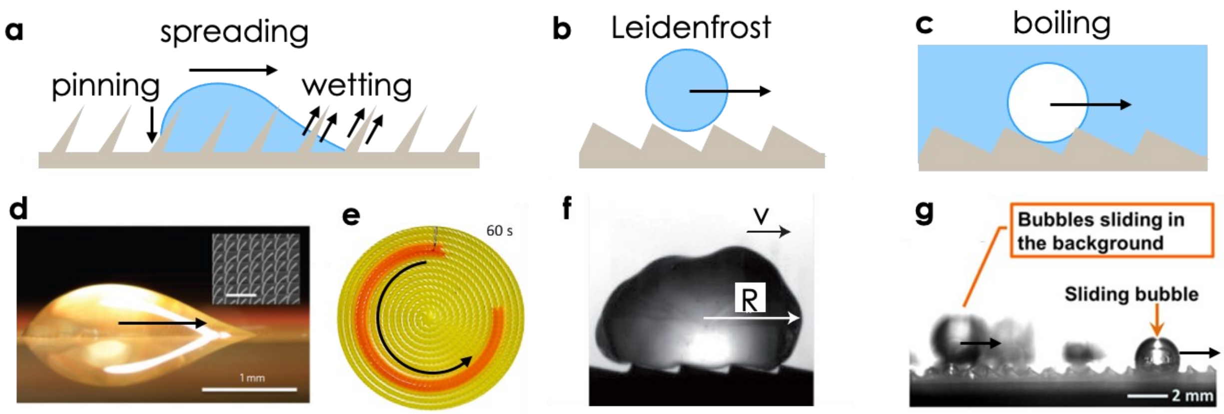

Figure 2. Droplet/Bubble mobility on asymmetric surface structures. Schematic of: a, Directional spreading of liquid. b, Directional transport of Leidenfrost droplet. c, Directional transport of vapor bubbles during boiling. d, Side-view image of a liquid spreading along the tilting direction of micropillars. Adapted with permission from reference [12]. Copyright 2010 Nature Portfolio. e, Top-down image of directional liquid spreading on a bio-inspired 3-dimensional asymmetric surface. Adapted with permission from reference [16]. Copyright 2021 American Association for the Advancement of Science. f, Leidenfrost droplet moving on a ratchet surface. Adapted with permission from reference [20]. Copyright 2011 Nature Portfolio. g, Boiling bubbles moving towards the right on an asymmetric surface in microgravity. Adapted with permission from reference [25]. Copyright 2015 The American Society of Mechanical Engineers.

Apart from asymmetric surface structures, another approach is to use asymmetric surface chemistry (i.e., a spatial gradient of surface energy) to manipulate droplet and bubble dynamics.[26,27] In theory, droplets would spontaneously move towards the more hydrophilic side to minimize the total surface energy of the system, while bubbles would move towards the more hydrophobic side. Many studies have designed surfaces with a wettability gradient through precise control of a coating with a molecular gradient.[28–32] For example, Chaudhury and Whitesides exposed a silicon substrate to the diffusing front of a decyltrichlorosilane vapor, and the resulting surface displayed a wettability gradient and can move a droplet uphill.[28] Zhang et al.

demonstrated fast droplets removal from a gradient quasi-liquid surface as small liquid droplets are continuously sprayed onto the surface.[29] For condensation heat transfer, both simulations[30,31] and experiments[32] of self-propelled dropwise condensation on a gradient surface have been reported. More experimental studies are needed to further investigate the heat transfer enhancements for condensation and for boiling, and the durability of these surfaces in terms of degradation and contamination.

Engineered nucleation sites

Controlling heterogeneous nucleation offers the capability to initiate nucleation and control the spatial distribution of the nucleated phase. In boiling, vapor bubbles tend to first nucleate on hydrophobic spots or cavities. This is because a vapor embryo on a hydrophobic spot or cavity has a lower curvature and thus a lower Laplace pressure compared to an equal-volume vapor embryo on a hydrophilic surface (**Figure 3a**). This translates to a reduced threshold wall temperature or superheat for the embryo to continue growing in size since the wall temperature needs to exceed the saturation temperature corresponding to the vapor pressure of the embryo.[3] Hsu developed a model that predicts the upper and lower bounds of active nucleation sites as a function of wall superheat.[33] Artificial nucleation cavities[34,35(p72),36], bi-philic surfaces,[37,38] and bi-thermal-conductive[39] surfaces have been developed to promote the onset of nucleate boiling (ONB), enhance boiling heat transfer coefficient (HTC), and enhance the critical heat flux (CHF). Hydrophilic artificial nucleation sites are also able to promote condensation nucleation. For example, Hou et al. developed a bi-philic surface with hydrophilic SiO_2 micropillars for controlled droplet nucleation and superhydrophobic nanostructured background for promoting drop-wise condensation and droplet departure.[36] As shown in **Figure 3b**, droplets only nucleate on the hydrophilic SiO_2, which allows precise control of the nucleation density for optimum thermal transport. Hoque et al. showed that proper design of the biphilic surface can significantly enhance the condensation heat transfer performance.[40] Recent works also demonstrated various strategies to fabricate scalable biphilic surfaces.[41,42] Artificial nucleation cavities have also been incorporated to enhance HTC in flow boiling where boiling occurs inside micro and mini channels.[43] Recently, anti-icing surfaces utilizing controlled nucleation of ice on sacrificial structures have been developed.[44] These anti-icing surfaces have ridge structures that favor ice nucleation because of the high local supersaturation, which effectively protects the substrate from nucleating ice.

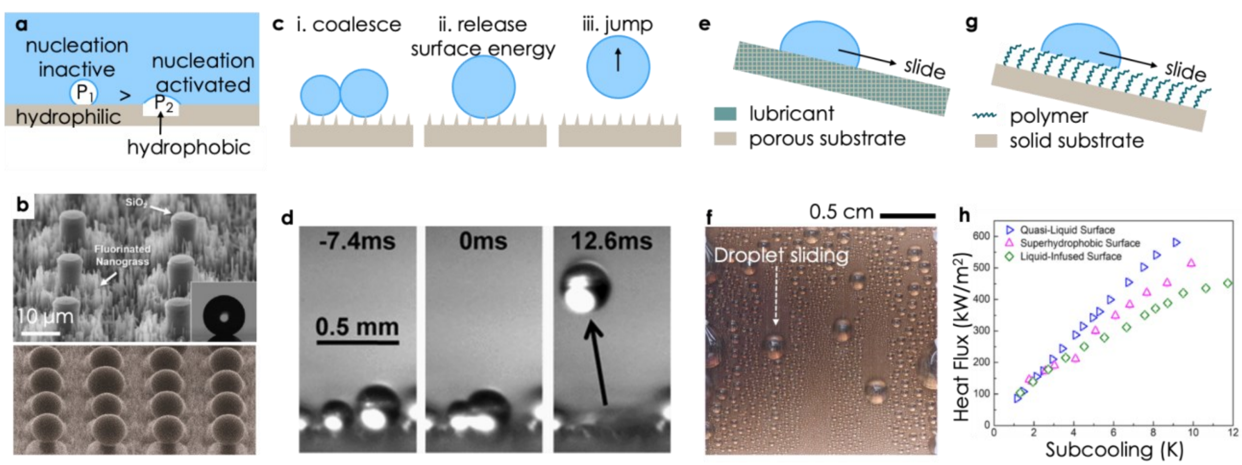

Figure 3. Examples of passive approaches to manipulate droplet and bubble dynamics for phase change applications. a, Schematic of bubble nucleation on an engineered nucleation site compared with a bubble nucleating on a hydrophilic surface. For the same initial bubble volume, the bubble in the hydrophobic

cavity has a lower curvature and a lower Laplace pressure. b, SEM image of a bi-philic surface. The top surfaces of micropillars are hydrophilic which serve as nucleation sites for condensation. The background is a superhydrophobic nanostructured surface that promotes drop-wise condensation. Adapted with permission from reference [36]. Copyright 2015 American Chemical Society. c, Schematic of coalesce-induced jumping droplet for condensation. d, Side-view images of drop removal via coalescence-induced jumping. Adapted with permission from reference [45]. Copyright 2009 American Physical Society. e, Schematic of dropwise condensation on slippery liquid-infused porous surfaces (SLIPS). f, Dropwise condensation on lubricant-infused vertical graphene nanoscaffolds. Adapted with permission from reference [46]. Copyright 2021 American Chemical Society. g, Schematic of dropwise condensation on quasi-liquid surfaces. h, Heat transfer characteristics of quasi-liquid surface, superhydrophobic surface, and liquid-infused surface. Adapted with permission from reference [47]. Copyright 2022 American Chemical Society.

Coalesce-induced jumping droplets on superhydrophobic surfaces

In recent years, significant attention has focused on drop-wise condensation on hydrophobic surfaces, which exhibit a much-improved heat transfer coefficient than conventional film-wise condensation on hydrophilic surfaces. In dropwise condensation, condensate droplets need to be removed to allow for continuous heat transfer. On a typical hydrophobic surface, droplets grow to the millimeter scale (on the order of capillary length) and then shed when gravity overcomes surface tension pinning force, exposing the surface underneath for further droplet nucleation.

Superhydrophobic surfaces, on the other hand, have been shown to promote droplet departure at a micrometric diameter by allowing coalesced droplets to jump away (**Figure 3c**).[48,49] Boreyko and Chen[45] reported that the excess surface energy released during droplet coalescence can be converted to the kinetic energy of the droplet which can lead to an out-of-plane jumping motion at a speed as high as 1 m/s (**Figure 3d**). Miljkovic et al. performed heat transfer characterization on nanostructured superhydrophobic copper oxide surfaces.[50] They demonstrated that jumping droplets can lead to a 25% higher overall heat flux and 30% higher condensation heat transfer coefficient compared to hydrophobic drop-wise condensing surfaces at low supersaturation. Enright et al. combined experimental measurement of jumping droplets during condensation and numerical simulation to show that only a small portion of the available excess surface energy is convertible to kinetic energy.[51] The upper bound of jumping velocity was also predicted. Numerous studies have characterized jumping droplets during condensation on nanostructured surfaces.[52–55] As will be discussed in the next section, the jumping droplets are found to carry a net electrostatic charge, allowing the use of an external electric field to prevent returning of these droplets to the surface to further enhance condensation heat transfer. Besides condensation, jumping droplets are also used in thermodiodes[9], water harvesting[56], anti-fogging[57], and vapor chambers for electronics cooling.[58,59]

However, the nanostructured superhydrophobic surfaces for jumping droplets tend to degrade easily over prolonged exposure to steam. A range of degradation mechanisms, both physical and chemical, have been reported such as clogging, erosion, and delamination.[60,61] The surface degradation results in hydrophilic defects which will transition jumping droplet condensation to film-wise condensation and lower the heat transfer coefficient (HTC). In addition, nanostructured superhydrophobic surfaces cannot achieve dropwise condensation for low surface tension fluids such as common refrigerants and natural gas liquids, which are widely applied in thermal management, refrigeration, and natural gas processing applications.

Liquid infused surfaces and quasi-liquid surfaces for condensation and anti-icing
The challenges associated with superhydrophobic surface degradation and the difficulty to achieve drop-wise condensation for low-surface tension fluids motivate the development of slippery liquid-infused porous surfaces (SLIPS) or liquid-infused surfaces (LIS). SLIPS or LIS consists of a lubricating film within a porous solid material (**Figure 3e**).[62–64] LIS enables minimal droplet adhesion, high droplet mobility, and dropwise condensation of low-surface-tension fluids, all of which are beneficial for enhanced condensation heat transfer for various fluids[65–67]. For example, Tripathy et al. studied enhanced dropwise condensation on lubricant-infused vertical graphene nanoscaffolds (**Figure 3f**).[46] SLIPS also offers anti-icing functionalities because condensed droplets or ice shed easily.[68–70] Recent development in SLIPS are summarized in a few reviews.[68,71] It is worth mentioning that depending on the surface energy of the solid, lubricant, and the liquid droplet, the lubricant can cloak the droplet, causing the lubricant to gradually deplete as droplets are removed. In addition, lubricant can be collected along with the condensed liquid due to cloaking, which is not desired in certain applications. Several other failure mechanisms of LIS such as displacement of the lubricant by the impinging fluid, miscibility of the impinging fluid and the lubricant, and incomplete wetting of the lubricant in the porous substrate for condensation applications are discussed in recent works.[66,67] Furthermore, Hoque et al. experimentally investigated the effect of cloaking and lubricants viscosities on the lifespan of LIS and outlined the design guidelines of LIS for different working environments.[72]

Quasi-Liquid Surfaces (QLS), on the other hand, are shown to address the durability/liquid depletion challenges faced by Liquid Infused Surfaces (LIS).[73,74,47] These surfaces are made by covalently bonding flexible polymer molecules to solid substrates (**Figure 3g**). These molecules have mobile chains on the untethered end and behave similarly to the lubricant layer to allow low droplet adhesion and contact angle hysteresis. Owing to the robust chemical bonding of the polymer to the substrate, QLS can avoid the issue of miscibility, cloaking and drainage observed in LIS. For example, Zhang et al. tethered polydimethylsiloxane (PDMS) on a solid silicon substrate and demonstrated an ultralow contact angle hysteresis of only 1 ° with water (substrate at 105 °C).[73] Further, fog harvesting experiments were conducted on the quasi-liquid surface and no obvious degradation was observed after 253 minutes. Cha et al. demonstrated stable dropwise condensation of water on a hydrophilic PEGylated silicon surface with minimal contact angle hysteresis (< 3 °).[74] Monga et al. characterized the condensation heat transfer performance and showed that the quasi-liquid surface outperformed the LIS and superhydrophobic surfaces (**Figure 3h**).[47]

Dynamic manipulation
While static surface structures and chemistry provide an appreciable tuning capability of multiphase fluid for thermal applications, dynamically tunable wetting systems enable even wider functionalities and real-time control capability. These dynamically tunable systems generally utilize structures and chemistries that respond to electrical, thermal, optical, chemical, and magnetic stimuli to manipulate wettability. The key metrics are response time, the energy required for the stimuli, reversibility, and tuning range (such as the change of contact angle). This section will cover a few approaches relevant to thermal applications using

electric fields (electrowetting, electric field-enhanced jumping droplet, ionic surfactants in an electric field) and light (photo-thermal capillary effect, photo-sensitive surfactants).

Electrowetting

Electrowetting and in particular electrowetting-on-dielectric (EWOD) have been successfully applied to manipulate wetting behavior for digital microfluidics and phase-change thermal applications. Electrowetting is a phenomenon where the wettability or the contact angle of a surface is controlled by an applied electric potential between the solid and a liquid.[48] The mechanism of electrowetting can be understood as a force generated by the electric field pulling droplets towards the substrate, which lowers the contact angle (**Figure 4a**). Conventionally, the liquid is in contact with a metallic electrode substrate, and EWOD refers to electrowetting on an electrode with a dielectric layer to prevent electrochemical reactions.

Electrowetting and EWOD have found wide applications including digital microfluidics[76,77], tunable lenses[78], energy harvesting[79], MEMS actuators[80], thermal switch[81], and phase change thermal transport.[82,83] Digital microfluidics is realized on an array of electrodes where voltages are dynamically controlled to transport, split and merge liquid droplets [76,77]. It is based on the mechanism that a droplet contacting two electrodes can have different contact angles according to the voltage applied to each electrode (**Figure 4b**). This results in an unbalanced surface tension along the surface direction pulling droplets towards the lower contact angle side. For thermal applications, electrowetting has been shown to trigger early bubble departure at the onset of nucleate boiling (ONB) and enhance the CHF by destabilizing the vapor film during pool boiling.[84] Electrowetting has also been used to transport liquid droplets in heat pipes [85–87] for thermal management (**Figure 4c**). The change of contact angle during electrowetting allows droplets to contact and detach from a heat transfer surface, and the device functions as a thermal switch (**Figure 4d**).[81,88] Electrowetting is generally simple to implement and can achieve a fast response time (~ 0.02-1 s),[89,90] large changes in the contact angle, and good reversibility. However, it usually requires a high voltage (several hundred volts) and a microfabricated electrode array.

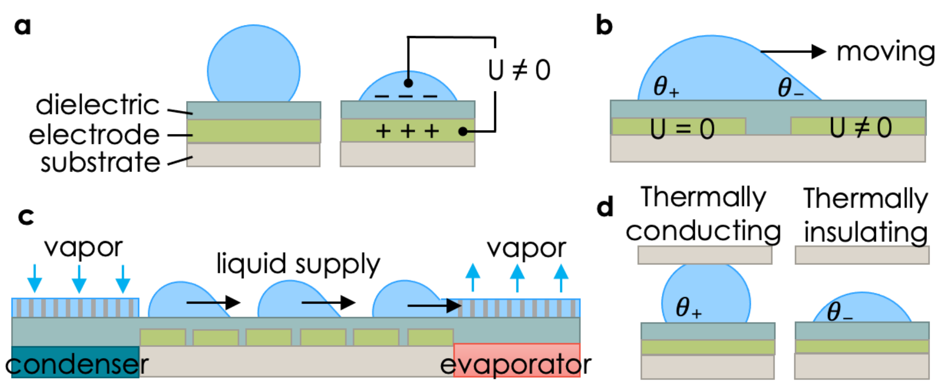

Figure 4. Application of electrowetting in thermal systems. a, Electrowetting on dielectrics. b, Droplet transport on an electrode array. c, Using electrowetting for liquid transport in heat pipes. d, Electrowetting for thermal diodes.

Electric-field-enhanced (EFE) jumping droplets

Recent works on condensation have reported that an external electric field can assist the removal of condensate droplets on superhydrophobic surfaces and therefore enhance the condensation heat transfer coefficient. As introduced earlier, during droplet coalescence, the release of excess surface energy enables the coalesced droplet to jump away from the superhydrophobic substrate. Miljkovic et al. showed that the jumping droplets gain a net positive charge which is associated with the formation of the electric double layer at the droplet-substrate interface and the subsequent swift charge separation during droplet jumping (**Figure 5a**).[91] They first observed that the jumping droplets repel each other mid-flight, and hypothesized that the jumping droplets have an electrostatic charge with the same charge polarity (**Figure 5b**). They further verified that the droplets are positively charged by introducing an external electrode with a positive and a negative bias, and by observing the trajectory of droplets in the presence of the electrode. The charge of droplets measured in a uniform electric field was shown to be constant for small droplets and proportional to the interfacial area between the droplet and the substrate. Based on this phenomenon, Miljkovic et al. further applied an external electric field to aid the removal of condensed droplets by preventing them from returning to the substrate due to the vapor flow towards the condensing surface (**Figure 5c**).[92] The external electrode has a negative bias which attracts the positively charged droplets. A 50% enhancement in the overall condensation heat transfer coefficient on a superhydrophobic surface was observed compared to that with no applied electric field for low supersaturations (**Figure 5c**). Birbarah et al. developed a detailed model to optimize the electrodes to minimize energy input based on the condensation heat flux.[93] In addition to a static electric field, Yan et al. reported enhanced droplets departure from superhydrophobic surfaces using an AC electric field parallel to the substrate.[94] Different from the droplet coalesce mechanism, the droplets stretch and recoil in the AC electric field which results in droplet jumping.

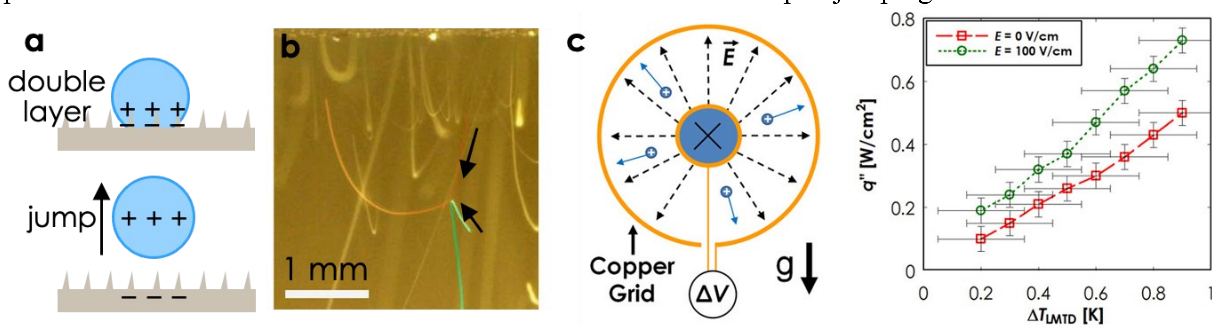

Figure 5. Electric-field-enhanced (EFE) jumping droplets. a, Charge separation during droplet departure results in a net positive charge. b, Long exposure time false-color images of droplet-droplet repulsive interactions. Arrows indicate the initial droplets trajectory. Adapted with permission from reference [91]. Copyright 2013 Nature Portfolio. c, Schematic of electric-field-enhanced jumping-droplet condensation and the heat transfer performance. Adapted with permission from reference [92]. Copyright 2013 American Chemical Society.

Electric-field-enhanced (EFE) jumping droplets are also used in applications beyond condensation. For example, Oh et al. utilized EFE jumping droplets for active cooling of electronics hot spots. The active spots of the electronics which generate localized heat are also applied upon a negative electric bias, thus directing the positively charged droplets to only cool the hot regions.[95] Miljkovic et al. demonstrated energy harvesting based on EFE jumping droplets, where the electrostatic charge from jumping condensate droplets is collected using another metal surface.[96] Traipattanaku et al. used EFE jumping droplets to demonstrate a thermal diode with a maximum thermal rectification of 325 using a voltage of 50 V.[10] Since EFE jumping droplets typically require a nanoengineered superhydrophobic surface, the degradation of these surfaces under prolonged condensation remains a key challenge which requires further research efforts.

Ionic surfactants in an electric field

An alternative approach to tuning multiphase systems is to use surfactants since they affect the surface tension or interfacial tension. Recent works have demonstrated active control of the contact angle using ionic surfactants and electric fields.[7,97] Ionic surfactants with a positive or negative charge on the hydrophilic end can adsorb to or desorb from a solid electrode surface when a potential is applied, therefore changing the solid-liquid interfacial tension on demand. For example, a positively-charged surfactant can be attracted to an electrode with a negative potential, aligning the hydrophobic tails towards the liquid phase which effectively makes the solid surface more hydrophobic. When a positive potential is applied, the positively-charged surfactants are repelled from the solid which then becomes less hydrophobic. The advantage of this approach compared to electrowetting is a significantly reduced activation voltage, which is only 1-3 V, as compared to ~ 100-1000 V in electrowetting. The response time is slightly slower, about 0.5 s.[7] Similar to electrowetting, prefabricated electrodes are needed to realize spatial control. The spatial resolution of such an approach is limited to the size of an electrode.

Cho et al. applied this principle to actively control the onset of nucleate boiling.[97] An array of electrodes was fabricated on a boiling substrate with constant heat flux and charged surfactants were added to the water. When a small electric potential (< 2 V) is applied to an electrode that adsorbs surfactants, nucleate boiling immediately occurs because the contact angle in the liquid phase increases which lowers the Laplace pressure required to activate nucleation. When the potential is reversed, surfactants desorb from the electrode which makes the surface to be relatively hydrophilic again, and nucleate boiling subsides. They demonstrated the ability to turn boiling on and off on demand and with spatial control. Li et al.[7] further applied ionic surfactants for digital microfluidics where droplet splitting, transport, and merging were demonstrated on an array of electrodes. They report that, by electrostatically adsorbing surfactants to the substrate, the contact angle of various liquids changes up to 60 degrees.

Light-controlled Thermal-capillary effect

The above three methods all use an electric field as the external stimulus. Here we introduce bubble/droplet manipulation controlled by light. The advantages of a light-controlled system include a potential spatial resolution down to the diffraction limit and real-time reconfigurability as no pre-made electrodes are required. One of the most widely studied phenomena which can be activated by light is the thermal-capillary effect.[98] Thermal-capillary effect drives fluid motion by utilizing a temperature gradient surrounding a bubble or a droplet, which results in a surface tension gradient causing the Marangoni flow. The Marangoni flow exerts a net force on the droplet or bubble which causes it to move.[99] Note that thermal-capillary effect is initiated by a temperature gradient and does not necessarily need a light source as the heating method.[100,101] However, photo-thermal capillary effect uses light (usually laser) which can precisely heat a specific region around a bubble or droplet and it is easily programmable and reconfigurable.

Several studies have demonstrated bubble movement on a solid surface or nanoparticle suspensions directed by light, where the solid surface or nanoparticles are used to absorb light to generate heat. [11,102–104] Recent works have also shown that the depinning of the three-phase contact line near the laser source due to evaporation can also trigger the bubble to move (**Figure 6a-b**).[104–106] This mechanism works in conjunction with the thermal-capillary effect to drive a surface bubble (where there is a three-phase contact line) to move towards the higher temperature side. Yang et al.[107] further engineered 'active surfactants' using functionalized nanoparticle dimers that respond to several external stimuli to drive droplet movement. The nanoparticles are light-absorbing and the thermal-capillary effect causes the droplet to move under a laser with an intensity of approximately 200 W/cm^2. The light intensities used in these studies range from 5.3 W/cm^2 (reference[11]) to 3.75 kW/cm^2 (reference[105]). Typically, light intensities on the order of 0.1-1 kW/cm^2 are used to drive bubble movement. The required temperature gradient depends on how the surface tension of different fluids shifts with temperature.

There have been limited studies using the thermal capillary effect for heat transfer applications because, without light control, the thermal capillary effect appears to hinder boiling heat transfer. During boiling, the heated surface has a higher temperature than the bulk fluid. The induced Marangoni flow, in this case, is away from the bubble base along the liquid-vapor interface causing the bubble to pin on the surface. As discussed earlier, delayed bubble departure can cause premature CHF. Zou et al. also reported that the thermal capillary effect causes the microlayer underneath a bubble to dry out during pool boiling.[108] Nevertheless, it is possible to use the light-controlled thermal capillary effect to precisely direct droplet and bubble motions for boiling, condensation, and other thermal applications.

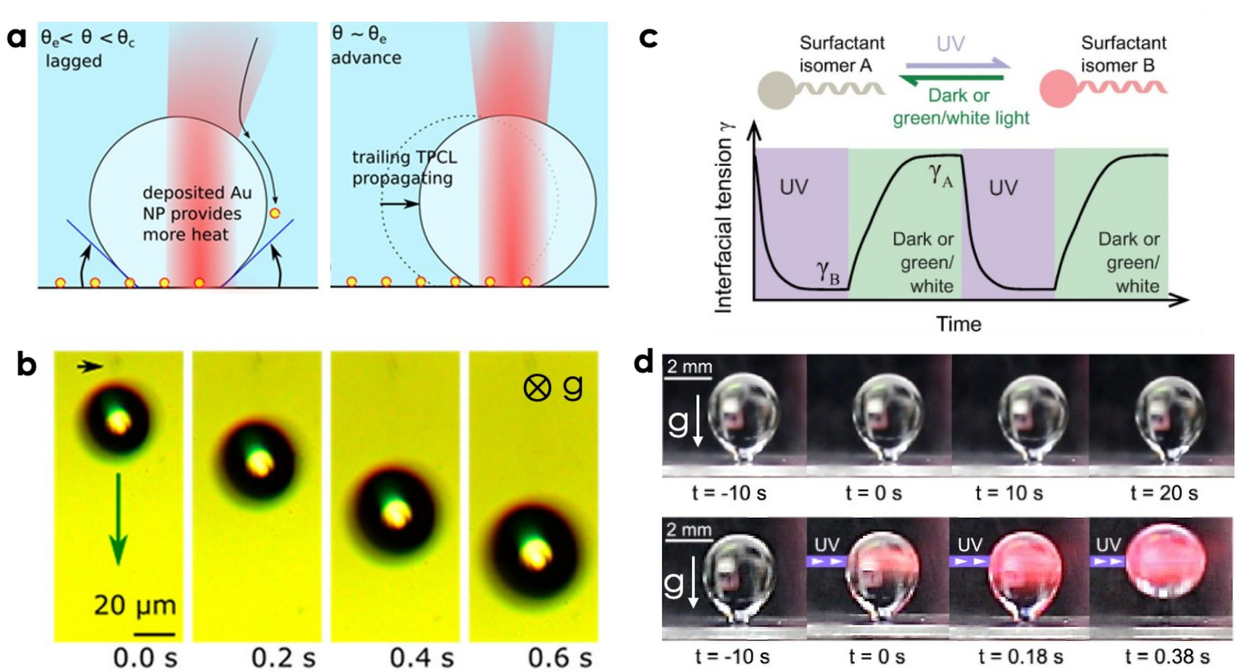

Figure 6. Thermal- and photo-capillary-induced droplet and bubble movement. a, Schematic of thermo-capillary effect wherein the deposited nanoparticles absorb laser heat. As a result, the evaporating three-phase contact line (TPCL) advances causing the bubble to move. b, Top-down optical images of bubble movement directed by thermal capillary effect. Adapted with permission from reference [104]. Copyright 2019 American Chemical Society. c, Photo-sensitive surfactants switch their molecular conformation upon light illumination, which causes a dynamic surface tension change. d, Time-lapse images of a droplet without and with laser illumination. The laser enabled the droplet to depart from the surface in 0.38 s. Adapted with permission from reference [109]. Copyright 2022 American Chemical Society.

Photo-Marangoni effect

More recently, photo-responsive surfactants have been used to create Marangoni flow which drives bubble or droplet movement. Photo-responsive surfactants change their molecular conformation upon light illumination, which can cause a change in the surface tension or interfacial tension. This creates a Marangoni flow along a fluid-fluid interface, which exerts a net force on the droplet or bubble. Like the photo-thermal effect, this approach does not require nanofabrication to realize spatial control and only requires a low light intensity to initiate photoswitch. The stability and reversibility of the surfactants and the reaction kinetics that determines the response timescale are important parameters to tune and optimize. So far, some of the photo-responsive surfactants are not stable in an aqueous or pH-neutral environment or can degrade when in contact with oxygen. The timescale of the photoswitch of common photo-responsive surfactants is usually 1-10 s, much slower than EWOD and slower than ionic surfactants in an electric field. However, this timescale has the potential to be reduced by tuning the chemistry of the surfactants.

Photo-surfactants have recently been used for manipulating micro/nanoparticles and drops in liquid solutions, by inducing a converging flow at a designated spot.[110–112] More recently, Lei et al. demonstrated droplet and bubble departure from a solid substrate using photo-responsive surfactants (**Figure 6c-d**).[109] The change of surface tension increases with light intensity, however, the maximum intensity used to depart droplets and bubbles is 44 mW/mm^2 or 4.4 W/cm^2, much lower than the intensity needed in thermal-Marangoni-driven bubble departure or depinning. Due to light absorption from the surfactants, it is possible for the light to heat the fluid. The change of surface tension due to heating is usually very small compared to the change of surface tension due to photoswitch. In some cases, heating causes the surface tension to decrease whereas the photo-switch increases the surface tension, which ultimately drives the fluid motion. The photo-Marangoni effect can potentially be widely applied to multi-phase fluid applications including digital microfluidics and lab-on-a-chip platforms. Its application in phase change heat transfer remains to be investigated. Mainly, to realize boiling, faster reaction kinetics (~ 50 ms) is required.

Discussion and Conclusion

The static droplet and bubble manipulation techniques discussed in this review offer a wide range of enhancements in heat transfer coefficient, critical heat flux, and directional mobility. In addition, the static techniques utilizing asymmetric surface structures and chemistry for directional mobility have a potential for both terrestrial and microgravity applications. It is to be noted that the durability of the introduced engineered surface structures and chemistries is of extreme importance to achieve prolonged efficient phase change heat transfer, especially for drop-wise condensation, which typically needs a hydrophobic coating on an intrinsically hydrophilic metal substrate.[60,113] Therefore, phase change heat transfer measurements on engineered surfaces should include long-term tests, if possible. To overcome durability challenges, recent works have investigated robust surface coatings such as metal-polymer composites,[114–116] self-healing coatings,[117] corrosion-resistant coatings[118,119], as well as robust hierarchical surface structures.[120] Another important consideration for industrial applications is scalability. As such, scalable manufacturing methods such as chemical etching and oxidation[121] and sandblasting[122] have recently been developed to obtain required surface morphologies. Furthermore, an emerging area of interest is to utilize additive manufacturing to engineer micro and macro structures for thermal applications.[123–126]

While useful, static manipulation techniques lack real-time control and tunability which is often desired in practical applications. The dynamic methods, while consuming external energy, allow for tunable droplet/bubble manipulation. The dynamic strategies discussed in this paper offer a multitude of spatial resolution, response times, and external energy requirements. Electrowetting offers the fastest response time (~ 0.02-1 s), whereas chemical methods such as photo-responsive surfactants could be slow (~ seconds), depending on the specific reaction kinetics. The prospect of being able to alter the reaction kinetics makes the chemical methods a very attractive avenue for future research. System stability is another important consideration. For example, the durability of superhydrophobic nanostructures for electric-field-enhanced jumping-droplet condensation, and the stability of photo-responsive surfactants in various chemical and thermal environments are both important for the longevity of the system. Most dynamic methods require external stimuli, which may consume energy. Voltage-wise, electrowetting needs the highest activation voltage (~ 100-1000 V), followed by electric-field-enhanced jumping-droplet condensation, while the ionic surfactants require the lowest voltage (~ 2 V). The requirement for light intensity is higher for the thermal-capillary effect than for the photo-capillary effect. For spatial resolution, light-activated systems can theoretically offer a resolution down to the diffraction limit, and real-time reconfiguration of the optical pattern. However, the system would require optical access. Electrically-controlled systems would require nanofabrication of microelectrode arrays to achieve high spatial resolution, which can be complex however such systems do not require a sophisticated optical source and optical access.

Other dynamic manipulation mechanisms based on thermal[127], magnetic[128,129], chemical[130,131], and mechanical stimulations[132] have also been reported in the literature. Most dynamic methods have only been shown to manipulate wettability and liquid/bubble transport, yet their applications to thermal and other systems remain to be fully explored, which presents new research and development opportunities. For example, new photo-surfactants with fast switching kinetics, good solubility in various thermal fluids, and long-term stability can be developed to tune boiling, condensation, and even gas-forming electrocatalysis which have fast time scales. In particular, responsive surfactants soluble in lubricants may be used in LIS to manipulate droplets for condensation and anti-icing applications. Non-toxic, bio-compatible responsive surfactants also need to be developed for water based applications.

Acknowledgments
This work was supported by the National Science Foundation and Center for the Advancement of Science in Space NSF-CASIS Transport Phenomena grant no. 2025655. V. Kumar acknowledges funding support from the National Science Foundation under the award number 2047727. F. Ahmadi acknowledges funding support from the UCSB Institute for Energy Efficiency.

Disclosure
The authors declare no conflict of interest.

References:
1. Wiser W. *Energy Resources - Occurrence, Production, Conversion, Use*. 1st ed. Springer-Verlag New York; 2000. Accessed December 27, 2017. //www.springer.com/us/book/9780387987446
2. Lawrence Livermore National Laboratory Flow Charts,

2021.https://flowcharts.llnl.gov/commodities/energy.
3. Cho HJ, Preston DJ, Zhu Y, Wang EN. Nanoengineered materials for liquid–vapour phase-change heat transfer. *Nat Rev Mater*. 2016;2:16092. doi:10.1038/natrevmats.2016.92
4. Lu Z, Zhu W, Yu X, et al. Ultrahigh Hydrogen Evolution Performance of Under-Water “Superaerophobic” MoS2 Nanostructured Electrodes. *Advanced Materials*. 2014;26(17):2683-2687. doi:10.1002/adma.201304759
5. A. Kempler P, P. Ifkovits Z, Yu W, I. Carim A, S. Lewis N. Optical and electrochemical effects of H 2 and O 2 bubbles at upward-facing Si photoelectrodes. *Energy & Environmental Science*. 2021;14(1):414-423. doi:10.1039/D0EE02796K
6. Iwata R, Zhang L, Wilke KL, et al. Bubble growth and departure modes on wettable/non-wettable porous foams in alkaline water splitting. *Joule*. 2021;5(4):887-900. doi:10.1016/j.joule.2021.02.015
7. Li J, Ha NS, Liu T ‘Leo,’ van Dam RM, ‘CJ’ Kim CJ. Ionic-surfactant-mediated electro-dewetting for digital microfluidics. *Nature*. 2019;572(7770):507-510. doi:10.1038/s41586-019-1491-x
8. Honda S, Minagawa Y, Noji H, Tabata KV. Multidimensional Digital Bioassay Platform Based on an Air-Sealed Femtoliter Reactor Array Device. *Anal Chem*. 2021;93(13):5494-5502. doi:10.1021/acs.analchem.0c05360
9. Boreyko JB, Zhao Y, Chen CH. Planar jumping-drop thermal diodes. *Appl Phys Lett*. 2011;99(23):234105. doi:10.1063/1.3666818
10. Traipattanakul B, Tso CY, Chao CYH. A phase-change thermal diode using electrostatic-induced coalescing-jumping droplets. *International Journal of Heat and Mass Transfer*. 2019;135:294-304. doi:10.1016/j.ijheatmasstransfer.2019.01.110
11. Hu W, Ishii KS, Ohta AT. Micro-assembly using optically controlled bubble microrobots. *Appl Phys Lett*. 2011;99(9):094103. doi:10.1063/1.3631662
12. Chu KH, Xiao R, Wang EN. Uni-directional liquid spreading on asymmetric nanostructured surfaces. *Nat Mater*. 2010;9(5):413-417. doi:10.1038/nmat2726
13. Wang Q, Yao X, Liu H, Quéré D, Jiang L. Self-removal of condensed water on the legs of water striders. *PNAS*. 2015;112(30):9247-9252. doi:10.1073/pnas.1506874112
14. Chen H, Zhang P, Zhang L, et al. Continuous directional water transport on the peristome surface of Nepenthes alata. *Nature*. 2016;532(7597):85-89. doi:10.1038/nature17189
15. Li J, Zhou X, Li J, et al. Topological liquid diode. *Science Advances*. 3(10):eaao3530. doi:10.1126/sciadv.aao3530
16. Feng S, Zhu P, Zheng H, et al. Three-dimensional capillary ratchet-induced liquid directional steering. *Science*. 2021;373(6561):1344-1348. doi:10.1126/science.abg7552
17. Lv C, Chen C, Chuang YC, et al. Substrate Curvature Gradient Drives Rapid Droplet Motion. *Phys Rev Lett*. 2014;113(2):026101. doi:10.1103/PhysRevLett.113.026101
18. Chen H, Ran T, Gan Y, et al. Ultrafast water harvesting and transport in hierarchical microchannels. *Nature Mater*. 2018;17(10):935-942. doi:10.1038/s41563-018-0171-9
19. Agapov RL, Boreyko JB, Briggs DP, et al. Asymmetric Wettability of Nanostructures Directs Leidenfrost Droplets. *ACS Nano*. 2014;8(1):860-867. doi:10.1021/nn405585m
20. Lagubeau G, Le Merrer M, Clanet C, Quéré D. Leidenfrost on a ratchet. *Nature Phys*. 2011;7(5):395-398. doi:10.1038/nphys1925
21. Linke H, Alemán BJ, Melling LD, et al. Self-Propelled Leidenfrost Droplets. *Phys Rev Lett*. 2006;96(15):154502. doi:10.1103/PhysRevLett.96.154502
22. Park KC, Kim P, Grinthal A, et al. Condensation on slippery asymmetric bumps. *Nature*. 2016;531(7592):78-82. doi:10.1038/nature16956
23. Dai X, Sun N, Nielsen SO, et al. Hydrophilic directional slippery rough surfaces for water harvesting. *Science Advances*. 4(3):eaaq0919. doi:10.1126/sciadv.aaq0919
24. Natesh S, Truong E, Narayanan V, Bhavnani S. Condensation on a horizontal surface with periodic asymmetrical structures – transient film growth. *International Journal of Heat and*

Mass Transfer. 2017;108:1126-1139. doi:10.1016/j.ijheatmasstransfer.2016.12.086
25. Thiagarajan N, Bhavnani SH, Narayanan V. Self-Propelled Sliding Bubble Motion Induced by Surface Microstructure in Pool Boiling of a Dielectric Fluid Under Microgravity. *Journal of Electronic Packaging*. 2015;137(2). doi:10.1115/1.4029246
26. Zheng Z, Yang H, Cao Y, Dai Z. Laser-Induced Wettability Gradient Surface of the Aluminum Matrix Used for Directional Transportation and Collection of Underwater Bubbles. *ACS Omega*. 2020;5(1):718-725. doi:10.1021/acsomega.9b03349
27. Bai H, Wang L, Ju J, Sun R, Zheng Y, Jiang L. Efficient Water Collection on Integrative Bioinspired Surfaces with Star-Shaped Wettability Patterns. *Advanced Materials*. 2014;26(29):5025-5030. doi:10.1002/adma.201400262
28. Chaudhury MK, Whitesides GM. How to Make Water Run Uphill. *Science*. 1992;256(5063):1539-1541. doi:10.1126/science.256.5063.1539
29. Zhang L, Guo Z, Sarma J, Zhao W, Dai X. Gradient Quasi-Liquid Surface Enabled Self-Propulsion of Highly Wetting Liquids. *Advanced Functional Materials*. 2021;31(13):2008614. doi:10.1002/adfm.202008614
30. Singh M, Kondaraju S, Bahga SS. Mathematical Model for Dropwise Condensation on a Surface With Wettability Gradient. *Journal of Heat Transfer*. 2018;140(7). doi:10.1115/1.4039014
31. Deng Z, Zhang C, Shen C, Cao J, Chen Y. Self-propelled dropwise condensation on a gradient surface. *International Journal of Heat and Mass Transfer*. 2017;114:419-429. doi:10.1016/j.ijheatmasstransfer.2017.06.065
32. Deng Z, Gao S, Wang H, Liu X, Zhang C. Visualization study on the condensation heat transfer on vertical surfaces with a wettability gradient. *International Journal of Heat and Mass Transfer*. 2022;184:122331. doi:10.1016/j.ijheatmasstransfer.2021.122331
33. Hsu YY. On the Size Range of Active Nucleation Cavities on a Heating Surface. *J Heat Transfer*. 1962;84(3):207-213. doi:10.1115/1.3684339
34. Hutter C, Kenning DBR, Sefiane K, et al. Experimental pool boiling investigations of FC-72 on silicon with artificial cavities and integrated temperature microsensors. *Experimental Thermal and Fluid Science*. 2010;34(4):422-433. doi:10.1016/j.expthermflusci.2009.03.010
35. Yu CK, Lu DC, Cheng TC. Pool boiling heat transfer on artificial micro-cavity surfaces in dielectric fluid FC-72. *J Micromech Microeng*. 2006;16(10):2092. doi:10.1088/0960-1317/16/10/024
36. Hou Y, Yu M, Chen X, Wang Z, Yao S. Recurrent Filmwise and Dropwise Condensation on a Beetle Mimetic Surface. *ACS Nano*. 2015;9(1):71-81. doi:10.1021/nn505716b
37. Betz AR, Jenkins J, Kim CJ “CJ”, Attinger D. ar. *Int J Heat Mass Transf*. 2013;57(2):733-741. doi:10.1016/j.ijheatmasstransfer.2012.10.080
38. Betz AR, Xu J, Qiu H, Attinger D. Do surfaces with mixed hydrophilic and hydrophobic areas enhance pool boiling? *Applied Physics Letters*. 2010;97(14):141909. doi:10.1063/1.3485057
39. Mahamudur Rahman M, Pollack J, McCarthy M. Increasing Boiling Heat Transfer using Low Conductivity Materials. *Scientific Reports*. 2015;5:13145. doi:10.1038/srep13145
40. Hoque MJ, Chavan S, Lundy R, et al. Biphilic jumping-droplet condensation. *Cell Reports Physical Science*. 2022;3(4):100823. doi:10.1016/j.xcrp.2022.100823
41. Hou Y, Shang Y, Yu M, Feng C, Yu H, Yao S. Tunable Water Harvesting Surfaces Consisting of Biphilic Nanoscale Topography. *ACS Nano*. 2018;12(11):11022-11030. doi:10.1021/acsnano.8b05163
42. Chehrghani MM, Abbasiasl T, Sadaghiani AK, Koşar A. Biphilic Surfaces with Optimum Hydrophobic Islands on a Superhydrophobic Background for Dropwise Flow Condensation. *Langmuir*. 2021;37(46):13567-13575. doi:10.1021/acs.langmuir.1c01844
43. Kandlikar SG, Kuan WK, Willistein DA, Borrelli J. Stabilization of Flow Boiling in Microchannels Using Pressure Drop Elements and Fabricated Nucleation Sites. *J Heat*

Transfer. 2005;128(4):389-396. doi:10.1115/1.2165208
44. Ahmadi SF, Nath S, Iliff GJ, et al. Passive Antifrosting Surfaces Using Microscopic Ice Patterns. *ACS Appl Mater Interfaces*. 2018;10(38):32874-32884. doi:10.1021/acsami.8b11285
45. Boreyko JB, Chen CH. Self-propelled dropwise condensate on superhydrophobic surfaces. *Phys Rev Lett*. 2009;103(18):184501. doi:10.1103/PhysRevLett.103.184501
46. Tripathy A, Lam CWE, Davila D, et al. Ultrathin Lubricant-Infused Vertical Graphene Nanoscaffolds for High-Performance Dropwise Condensation. *ACS Nano*. 2021;15(9):14305-14315. doi:10.1021/acsnano.1c02932
47. Monga D, Guo Z, Shan L, Taba SA, Sarma J, Dai X. Quasi-Liquid Surfaces for Sustainable High-Performance Steam Condensation. *ACS Appl Mater Interfaces*. 2022;14(11):13932-13941. doi:10.1021/acsami.2c00401
48. Wang S, Zhang W, Yu X, Liang C, Zhang Y. Sprayable superhydrophobic nano-chains coating with continuous self-jumping of dew and melting frost. *Sci Rep*. 2017;7(1):40300. doi:10.1038/srep40300
49. Liu F, Ghigliotti G, Feng JJ, Chen CH. Numerical simulations of self-propelled jumping upon drop coalescence on non-wetting surfaces. *Journal of Fluid Mechanics*. 2014;752:39-65. doi:10.1017/jfm.2014.320
50. Miljkovic N, Enright R, Nam Y, et al. Jumping-droplet-enhanced condensation on scalable superhydrophobic nanostructured surfaces. *Nano Lett*. 2013;13(1):179-187. doi:10.1021/nl303835d
51. Enright R, Miljkovic N, Sprittles J, Nolan K, Mitchell R, Wang EN. How Coalescing Droplets Jump. *ACS Nano*. 2014;8(10):10352-10362. doi:10.1021/nn503643m
52. Cha H, Xu C, Sotelo J, et al. Coalescence-induced nanodroplet jumping. *Phys Rev Fluids*. 2016;1(6):064102. doi:10.1103/PhysRevFluids.1.064102
53. Chen X, Patel RS, Weibel JA, Garimella SV. Coalescence-Induced Jumping of Multiple Condensate Droplets on Hierarchical Superhydrophobic Surfaces. *Sci Rep*. 2016;6(1):18649. doi:10.1038/srep18649
54. Liu X, Cheng P, Quan X. Lattice Boltzmann simulations for self-propelled jumping of droplets after coalescence on a superhydrophobic surface. *International Journal of Heat and Mass Transfer*. 2014;73:195-200. doi:10.1016/j.ijheatmasstransfer.2014.01.060
55. Mulroe MD, Srijanto BR, Ahmadi SF, Collier CP, Boreyko JB. Tuning Superhydrophobic Nanostructures To Enhance Jumping-Droplet Condensation. *ACS Nano*. 2017;11(8):8499-8510. doi:10.1021/acsnano.7b04481
56. Ma X, Wang Y, Wu H, Wang Y, Yang Y. Efficient water scavenging by cooling superhydrophobic surfaces to obtain jumping water droplets from air. *Sci Rep*. 2019;9(1):13784. doi:10.1038/s41598-019-50199-9
57. Mouterde T, Lehoucq G, Xavier S, et al. Antifogging abilities of model nanotextures. *Nature Mater*. 2017;16(6):658-663. doi:10.1038/nmat4868
58. Boreyko JB, Chen CH. Vapor chambers with jumping-drop liquid return from superhydrophobic condensers. *International Journal of Heat and Mass Transfer*. 2013;61:409-418. doi:10.1016/j.ijheatmasstransfer.2013.01.077
59. Foulkes T, Oh J, Sokalski P, et al. Jumping droplets electronics cooling: Promise versus reality. *Appl Phys Lett*. 2020;116(20):203701. doi:10.1063/5.0002537
60. Ho JY, Rabbi KF, Khodakarami S, Ma J, Boyina KS, Miljkovic N. Opportunities in Nano-Engineered Surface Designs for Enhanced Condensation Heat and Mass Transfer. *Journal of Heat Transfer*. 2022;144(5). doi:10.1115/1.4053454
61. Wang R, Jakhar K, Ahmed S, Antao DS. Elucidating the Mechanism of Condensation-Mediated Degradation of Organofunctional Silane Self-Assembled Monolayer Coatings. *ACS Appl Mater Interfaces*. 2021;13(29):34923-34934. doi:10.1021/acsami.1c08496
62. Wong TS, Kang SH, Tang SKY, et al. Bioinspired self-repairing slippery surfaces with

pressure-stable omniphobicity. *Nature*. 2011;477(7365):443-447. doi:10.1038/nature10447
63. Epstein AK, Wong TS, Belisle RA, Boggs EM, Aizenberg J. Liquid-infused structured surfaces with exceptional anti-biofouling performance. *Proceedings of the National Academy of Sciences*. 2012;109(33):13182-13187. doi:10.1073/pnas.1201973109
64. Dai X, Stogin BB, Yang S, Wong TS. Slippery Wenzel State. *ACS Nano*. 2015;9(9):9260-9267. doi:10.1021/acsnano.5b04151
65. Preston DJ, Lu Z, Song Y, et al. Heat transfer enhancement during water and hydrocarbon condensation on lubricant infused surfaces. *Scientific Reports*. 2018;8(1):540. doi:10.1038/s41598-017-18955-x
66. Preston DJ, Song Y, Lu Z, Antao DS, Wang EN. Design of lubricant infused surfaces. *ACS Appl Mater Interfaces*. 2017;9(48):42383-42392. doi:10.1021/acsami.7b14311
67. Sett S, Yan X, Barac G, Bolton LW, Miljkovic N. Lubricant-infused surfaces for low-surface-tension fluids: promise versus reality. *ACS Appl Mater Interfaces*. 2017;9(41):36400-36408. doi:10.1021/acsami.7b10756
68. Kreder MJ, Alvarenga J, Kim P, Aizenberg J. Design of anti-icing surfaces: smooth, textured or slippery? *Nat Rev Mater*. 2016;1(1):1-15. doi:10.1038/natrevmats.2015.3
69. Kim P, Wong TS, Alvarenga J, Kreder MJ, Adorno-Martinez WE, Aizenberg J. Liquid-Infused Nanostructured Surfaces with Extreme Anti-Ice and Anti-Frost Performance. *ACS Nano*. 2012;6(8):6569-6577. doi:10.1021/nn302310q
70. Liu C, Li Y, Lu C, Liu Y, Feng S, Liu Y. Robust Slippery Liquid-Infused Porous Network Surfaces for Enhanced Anti-icing/Deicing Performance. *ACS Appl Mater Interfaces*. 2020;12(22):25471-25477. doi:10.1021/acsami.0c05954
71. Villegas M, Zhang Y, Abu Jarad N, Soleymani L, Didar TF. Liquid-Infused Surfaces: A Review of Theory, Design, and Applications. *ACS Nano*. 2019;13(8):8517-8536. doi:10.1021/acsnano.9b04129
72. Hoque MJ, Sett S, Yan X, et al. Life Span of Slippery Lubricant Infused Surfaces. *ACS Appl Mater Interfaces*. 2022;14(3):4598-4611. doi:10.1021/acsami.1c17010
73. Zhang L, Guo Z, Sarma J, Dai X. Passive Removal of Highly Wetting Liquids and Ice on Quasi-Liquid Surfaces. *ACS Appl Mater Interfaces*. 2020;12(17):20084-20095. doi:10.1021/acsami.0c02014
74. Cha H, Vahabi H, Wu A, et al. Dropwise condensation on solid hydrophilic surfaces. *Science Advances*. 2020;6(2):eaax0746. doi:10.1126/sciadv.aax0746
75. Klarman D, Andelman D, Urbakh M. A Model of Electrowetting, Reversed Electrowetting, and Contact Angle Saturation. *Langmuir*. 2011;27(10):6031-6041. doi:10.1021/la2004326
76. Cho SK, Moon H, Kim CJ. Creating, transporting, cutting, and merging liquid droplets by electrowetting-based actuation for digital microfluidic circuits. *Journal of Microelectromechanical Systems*. 2003;12(1):70-80. doi:10.1109/JMEMS.2002.807467
77. Choi K, Ng AHC, Fobel R, Wheeler AR. Digital Microfluidics. *Annual Review of Analytical Chemistry*. 2012;5(1):413-440. doi:10.1146/annurev-anchem-062011-143028
78. Krogmann F, Monch W, Zappe H. Electrowetting for Tunable Microoptics. *Journal of Microelectromechanical Systems*. 2008;17(6):1501-1512. doi:10.1109/JMEMS.2008.2007256
79. Krupenkin T, Taylor JA. Reverse electrowetting as a new approach to high-power energy harvesting. *Nature Communications*. 2011;2(1):1-8. doi:10.1038/ncomms1454
80. Preston DJ, Anders A, Barabadi B, et al. Electrowetting-on-dielectric actuation of a vertical translation and angular manipulation stage. *Appl Phys Lett*. 2016;109(24):244102. doi:10.1063/1.4971777
81. Cha G, Kim CJ, Ju YS. Thermal conductance switching based on the actuation of liquid droplets through the electrowetting on dielectric (EWOD) phenomenon. *Applied Thermal Engineering*. 2016;98:189-195. doi:10.1016/j.applthermaleng.2015.11.098
82. Yan Z, Jin M, Li Z, Zhou G, Shui L. Droplet-Based Microfluidic Thermal Management

Methods for High Performance Electronic Devices. *Micromachines*. 2019;10(2):89. doi:10.3390/mi10020089
83. Jones TB. Electrohydrodynamically Enhanced Heat Transfer in Liquids—A Review. In: Irvine TF, Hartnett JP, eds. *Advances in Heat Transfer*. Vol 14. Elsevier; 1979:107-148. doi:10.1016/S0065-2717(08)70086-8
84. Sur A, Lu Y, Pascente C, Ruchhoeft P, Liu D. Pool boiling heat transfer enhancement with electrowetting. *International Journal of Heat and Mass Transfer*. 2018;120:202-217. doi:10.1016/j.ijheatmasstransfer.2017.12.029
85. Wikramanayake E, Hale R, Elam J, et al. Characterizing Microfluidic Operations Underlying an Electrowetting Heat Pipe on the International Space Station. In: American Society of Mechanical Engineers Digital Collection; 2019. doi:10.1115/IMECE2018-86223
86. Hale RS, Bahadur V. Electrowetting Heat Pipes for Heat Transport Over Extended Distances. *IEEE Transactions on Components, Packaging and Manufacturing Technology*. 2015;5(10):1441-1450. doi:10.1109/TCPMT.2015.2472363
87. Hale RS, Bahadur V. Electrowetting-based microfluidic operations on rapid-manufactured devices for heat pipe applications. *J Micromech Microeng*. 2017;27(7):075004. doi:10.1088/1361-6439/aa711f
88. McLanahan AR, Richards CD, Richards RF. A dielectric liquid contact thermal switch with electrowetting actuation. *J Micromech Microeng*. 2011;21(10):104009. doi:10.1088/0960-1317/21/10/104009
89. Supekar OD, Zohrabi M, Gopinath JT, Bright VM. Enhanced Response Time of Electrowetting Lenses with Shaped Input Voltage Functions. *Langmuir*. 2017;33(19):4863-4869. doi:10.1021/acs.langmuir.7b00631
90. Annapragada SR, Dash S, Garimella SV, Murthy JY. Dynamics of Droplet Motion under Electrowetting Actuation. *Langmuir*. 2011;27(13):8198-8204. doi:10.1021/la201322b
91. Miljkovic N, Preston DJ, Enright R, Wang EN. Electrostatic charging of jumping droplets. *Nat Commun*. 2013;4. doi:10.1038/ncomms3517
92. Miljkovic N, Preston DJ, Enright R, Wang EN. Electric-Field-Enhanced Condensation on Superhydrophobic Nanostructured Surfaces. *ACS Nano*. 2013;7(12):11043-11054. doi:10.1021/nn404707j
93. Birbarah P, Li Z, Pauls A, Miljkovic N. A Comprehensive Model of Electric-Field-Enhanced Jumping-Droplet Condensation on Superhydrophobic Surfaces. *Langmuir*. 2015;31(28):7885-7896. doi:10.1021/acs.langmuir.5b01762
94. Yan X, Li J, Li L, Huang Z, Wang F, Wei Y. Droplet condensation on superhydrophobic surfaces with enhanced dewetting under a tangential AC electric field. *Appl Phys Lett*. 2016;109(16):161601. doi:10.1063/1.4964762
95. Oh J, Birbarah P, Foulkes T, et al. Jumping-droplet electronics hot-spot cooling. *Appl Phys Lett*. 2017;110(12):123107. doi:10.1063/1.4979034
96. Miljkovic N, Preston DJ, Enright R, Wang EN. Jumping-droplet electrostatic energy harvesting. *Applied Physics Letters*. 2014;105(1):013111. doi:10.1063/1.4886798
97. Cho HJ, Mizerak JP, Wang EN. Turning bubbles on and off during boiling using charged surfactants. *Nat Commun*. 2015;6:8599. doi:10.1038/ncomms9599
98. Karbalaei A, Kumar R, Cho HJ. Thermocapillarity in Microfluidics—A Review. *Micromachines*. 2016;7(1):13. doi:10.3390/mi7010013
99. Young NO, Goldstein JS, Block MJ. The motion of bubbles in a vertical temperature gradient. *Journal of Fluid Mechanics*. 1959;6(3):350-356. doi:10.1017/S0022112059000684
100. Daniel S, Chaudhury MK, Chen JC. Fast Drop Movements Resulting from the Phase Change on a Gradient Surface. *Science*. 2001;291(5504):633-636. doi:10.1126/science.291.5504.633
101. Bjelobrk N, Girard HL, Bengaluru Subramanyam S, Kwon HM, Quéré D, Varanasi KK.

Thermocapillary motion on lubricant-impregnated surfaces. *Phys Rev Fluids*. 2016;1(6):063902. doi:10.1103/PhysRevFluids.1.063902
102. Ohta AT, Jamshidi A, Valley JK, Hsu HY, Wu MC. Optically actuated thermocapillary movement of gas bubbles on an absorbing substrate. *Appl Phys Lett*. 2007;91(7):074103. doi:10.1063/1.2771091
103. Armon N, Greenberg E, Layani M, Rosen YS, Magdassi S, Shpaisman H. Continuous Nanoparticle Assembly by a Modulated Photo-Induced Microbubble for Fabrication of Micrometric Conductive Patterns. *ACS Appl Mater Interfaces*. 2017;9(50):44214-44221. doi:10.1021/acsami.7b14614
104. Zhang Q, Pang Y, Schiffbauer J, et al. Light-Guided Surface Plasmonic Bubble Movement via Contact Line De-Pinning by In-Situ Deposited Plasmonic Nanoparticle Heating. *ACS Appl Mater Interfaces*. 2019;11(51):48525-48532. doi:10.1021/acsami.9b16067
105. Zhao C, Xie Y, Mao Z, et al. Theory and experiment on particle trapping and manipulation via optothermally generated bubbles. *Lab Chip*. 2013;14(2):384-391. doi:10.1039/C3LC50748C
106. Zheng Y, Liu H, Wang Y, et al. Accumulating microparticles and direct-writing micropatterns using a continuous-wave laser-induced vapor bubble. *Lab Chip*. 2011;11(22):3816-3820. doi:10.1039/C1LC20478E
107. Yang Z, Wei J, Sobolev YI, Grzybowski BA. Systems of mechanized and reactive droplets powered by multi-responsive surfactants. *Nature*. 2018;553(7688):313-318. doi:10.1038/nature25137
108. Zou A, Gupta M, Maroo SC. Origin, Evolution, and Movement of Microlayer in Pool Boiling. *J Phys Chem Lett*. 2018;9(14):3863-3869. doi:10.1021/acs.jpclett.8b01646
109. Zhao L, Seshadri S, Liang X, et al. Depinning of Multiphase Fluid Using Light and Photo-Responsive Surfactants. *ACS Cent Sci*. Published online January 13, 2022. doi:10.1021/acscentsci.1c01127
110. Venancio-Marques A, Baigl D. Digital Optofluidics: LED-Gated Transport and Fusion of Microliter-Sized Organic Droplets for Chemical Synthesis. *Langmuir*. 2014;30(15):4207-4212. doi:10.1021/la5001254
111. Lv C, Varanakkottu SN, Baier T, Hardt S. Controlling the Trajectories of Nano/Micro Particles Using Light-Actuated Marangoni Flow. *Nano Lett*. 2018;18(11):6924-6930. doi:10.1021/acs.nanolett.8b02814
112. Hayashita T, Kurosawa T, Miyata T, Tanaka K, Igawa M. Effect of structural variation within cationic azo-surfactant upon photoresponsive function in aqueous solution. *Colloid Polym Sci*. 1994;272(12):1611-1619. doi:10.1007/BF00664729
113. Ma J, Sett S, Cha H, Yan X, Miljkovic N. Recent developments, challenges, and pathways to stable dropwise condensation: A perspective. *Appl Phys Lett*. 2020;116(26):260501. doi:10.1063/5.0011642
114. Chang HC, Rajagopal MC, Hoque MJ, et al. Composite Structured Surfaces for Durable Dropwise Condensation. *International Journal of Heat and Mass Transfer*. 2020;156:119890. doi:10.1016/j.ijheatmasstransfer.2020.119890
115. Donati M, Lam CWE, Milionis A, et al. Sprayable Thin and Robust Carbon Nanofiber Composite Coating for Extreme Jumping Dropwise Condensation Performance. *Advanced Materials Interfaces*. 2021;8(1):2001176. doi:10.1002/admi.202001176
116. Wilke KL, Antao DS, Cruz S, et al. Polymer Infused Porous Surfaces for Robust, Thermally Conductive, Self-Healing Coatings for Dropwise Condensation. *ACS Nano*. 2020;14(11):14878-14886. doi:10.1021/acsnano.0c03961
117. Ma J, Porath LE, Haque MF, et al. Ultra-thin self-healing vitrimer coatings for durable hydrophobicity. *Nat Commun*. 2021;12(1):5210. doi:10.1038/s41467-021-25508-4
118. Cohen N, Dotan A, Dodiuk H, Kenig S. Superhydrophobic Coatings and Their Durability. *Materials and Manufacturing Processes*. 2016;31(9):1143-1155.

doi:10.1080/10426914.2015.1090600
119. Li H, Yu S, Hu J, Yin X. Modifier-free fabrication of durable superhydrophobic electrodeposited Cu-Zn coating on steel substrate with self-cleaning, anti-corrosion and anti-scaling properties. *Applied Surface Science*. 2019;481:872-882. doi:10.1016/j.apsusc.2019.03.123
120. Wang D, Sun Q, Hokkanen MJ, et al. Design of robust superhydrophobic surfaces. *Nature*. 2020;582(7810):55-59. doi:10.1038/s41586-020-2331-8
121. Muneeshwaran M, Wang CC. Superhydrophobic fins with inclined arrangement for enhancing energy saving of air-cooled wet heat exchangers. *International Journal of Heat and Mass Transfer*. 2021;178:121636. doi:10.1016/j.ijheatmasstransfer.2021.121636
122. Song Y, Wang C, Preston DJ, et al. Enhancement of Boiling with Scalable Sandblasted Surfaces. *ACS Appl Mater Interfaces*. 2022;14(7):9788-9794. doi:10.1021/acsami.1c22207
123. Collins IL, Weibel JA, Pan L, Garimella SV. A permeable-membrane microchannel heat sink made by additive manufacturing. *International Journal of Heat and Mass Transfer*. 2019;131:1174-1183. doi:10.1016/j.ijheatmasstransfer.2018.11.126
124. Ho JY, Fazle Rabbi K, Khodakarami S, et al. Tunable and Robust Nanostructuring for Multifunctional Metal Additively Manufactured Interfaces. *Nano Lett*. 2022;22(7):2650-2659. doi:10.1021/acs.nanolett.1c04463
125. Ho JY, Rabbi KF, Khodakarami S, et al. Ultrascalable Surface Structuring Strategy of Metal Additively Manufactured Materials for Enhanced Condensation. *Advanced Science*. n/a(n/a):2104454. doi:10.1002/advs.202104454
126. Elkholy A, Unlusoy C, Kempers R. Thermal performance of a two-phase loop thermosyphon with an additively manufactured evaporator. *Applied Thermal Engineering*. 2022;202:117692. doi:10.1016/j.applthermaleng.2021.117692
127. Chen L, Liu M, Lin L, et al. Thermal-responsive hydrogel surface: tunable wettability and adhesion to oil at the water/solid interface. *Soft Matter*. 2010;6(12):2708-2712. doi:10.1039/C002543G
128. Zhu Y, Antao DS, Xiao R, Wang EN. Real-Time Manipulation with Magnetically Tunable Structures. *Adv Mater*. 2014;26(37):6442-6446. doi:10.1002/adma.201401515
129. Timonen JVI, Johans C, Kontturi K, Walther A, Ikkala O, Ras RHA. A Facile Template-Free Approach to Magnetodriven, Multifunctional Artificial Cilia. *ACS Appl Mater Interfaces*. 2010;2(8):2226-2230. doi:10.1021/am100244x
130. Zarzar LD, Kim P, Aizenberg J. Bio-inspired Design of Submerged Hydrogel-Actuated Polymer Microstructures Operating in Response to pH. *Advanced Materials*. 2011;23(12):1442-1446. doi:10.1002/adma.201004231
131. Beebe DJ, Moore JS, Bauer JM, et al. Functional hydrogel structures for autonomous flow control inside microfluidic channels. *Nature*. 2000;404(6778):588-590. doi:10.1038/35007047
132. Wang J, Sun L, Zou M, et al. Bioinspired shape-memory graphene film with tunable wettability. *Science Advances*. 3(6):e1700004. doi:10.1126/sciadv.1700004

Biography:

Xichen Liang

Xichen Liang obtained her BS degree from the Ohio State University in 2018. She joined the University of California, Santa Barbara in the Chemical Engineering department as a PhD student in 2020 under the supervision of Prof. Yangying Zhu. Her current research focuses on the dynamic manipulation of fluid with photo-responsive surfactants to enhance heat transfer.

Yangying Zhu

Yangying Zhu is an Assistant Professor in the Mechanical Engineering department at the University of California, Santa Barbara. Her research combines fundamental understanding of heat and mass transfer with novel materials fabrication and characterization capabilities to address thermal management challenges of electronic devices, batteries, and electrocatalytic systems.